HAMMER PEENING WITH A PIEZO-ACTUATED TOOL FOR SURFACE FINISHING

MARTIN KOLOUCH, MARKUS WABNER, ROBIN KURTH
Fraunhofer-Institute for Machine Tools and Forming Technology IWU, Chemnitz, Germany

DOI: 10.17973/MMSJ.2017_12_201786

e-mail: martin.kolouch@iwu.fraunhofer.de

Low roughness of free-form surfaces represents a challenge in production of forming tools. In the industry, the free-form surface is grinded and polished manually. The technology of hammer peening has the capability to replace the time consuming handcraft by automated machining with high productivity and other positive effects, like increased hardness and compressive residual stress in the surface layer. This leads to a high wear resistance of the machined surface. The hammer peening can be conducted with a piezo-actuated tool. The high frequency of such a tool allows achieving higher productivity than other actuator principles used in hammer peening tools. In this paper, a piezo-actuated hammer peening tool working in its mechanical resonance is presented. Furthermore, a cross-domain model including the process, the mechanical and the electrical part of the tool is explained. This model is further used for optimization of the process and the tool. The functionality of the tool is demonstrated by machining results.

KEYWORDS
finishing, dynamics, piezoelectric, simulation, hammer peening

1 INTRODUCTION

The hammer peening technology has been developed for the last decade in order to machine surfaces with complex geometrical shapes automatically [Bleicher 2012]. In principle, the hammer peening can be classified as a partial forming technology that smooths the roughness by pressing a hard ball into the surface, see Figure 1.Hereby, plastic deformations are induced.Thus,the roughness after milling R_z' is reduced to a roughness after hammer peening R_z(usual from R_z' 10to R_z 2 µm) and the hammer print on the surface occurred. Furthermore, the plastic deformations cause a compressive residual stress, strain hardening and increased hardness (e.g. from 340 to 370 HV or from 370 to 470 HV) in a thin surface layer (up to 1 mm), as reported in [Groche 2009], [Adjassoho 2012], [Wied 2011],[Berglund 2011], [Groche 2012]. All these effectsincrease the wear resistance of the machined surface.In order to enable this machining result, the ball oscillates in axial tool direction driven by an actuator. After the pressing event (ball position at lower reversing point), the ball of the tooltakes off to the initial position and one cycle of the hammer peening process is finalized.

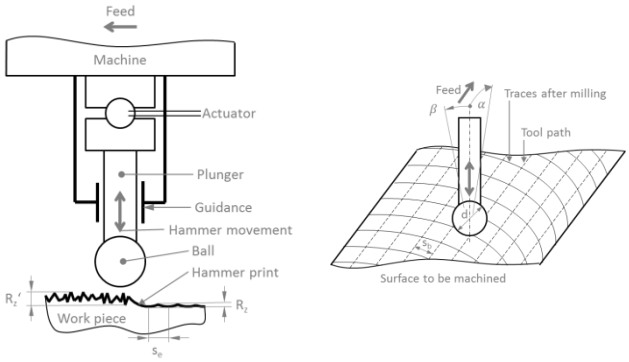

Figure 1. Principle of the hammer peening with basic process parameters

The next hammer print in a certain distance s_e from the previous one demands a movement of the tool with a constant feed velocity $v_f$along a tool path.The velocity $v_f$can be computed as follows

$$v_f = s_e f_{HP} \quad (1)$$

With f_{HP} being the constant frequency of the hammer movement.For the purpose of surface smoothing, the tool path has to be repeated in a distance s_b to the previous tool path (see Figure 1).Additionally, the tool can be tilted during machining by an angel α in a plane spanned by a vector of the feed direction and the normal vector of the surface being machined and/or by an angel β in the normal plane to the first plane and the surface.

The twoangles (α,β)just take influence on the surface quality like roughness, hardness etc. Furthermore, the parameters s_e and $s_b$essentially determine the roughness after hammer peening. Therefore, the frequency f_{HP} represents a crucial factor for increasing the hammer peening productivity, i.e. reducing machining time. In the face of the fact that hammer peening of a large forming tool can take a few days [Groche 2011], the need for the high productivity becomes obvious.

The frequency f_{HP} belongs to basic characteristics of a hammer peening tool (HPT). There are various HPT with different actuating principles, like pneumaticwith $f_{HP}\approx 200\text{-}300$ Hz [Wied 2011], electro-magnetic $f_{HP}<500$ Hz [Bleicher 2012] and piezoelectric $f_{HP}\approx 700$ Hz. This briefly overview shows the high potential of HPT with piezoelectric actuator for increasing the productivity. Thus, this kind of HPT is intensively researched at Fraunhofer IWU. In contrast to other actuating principles, the HPT with a piezoelectric actuator features very low rangefor the hammer movement. Considering deviations of the machine, workpiececlamping and tolerances of the workpiece, this small value could cause a strong limitation in application of this kind of HPT. Therefore, a HPT with a piezoelectric actuator requires a unit with defined compliance assembled between the machine and the HPT, which reduces the impact of these deviations on the machining results. In this paper, a novel HPT with piezoelectric actuator is presented. This tool works in its resonance frequency in order to reach maximal process force and minimal energy consumption.

2 DESIGN OF THE NOVEL PIEZOELECTRIC HAMMER PEENING TOOL

The novel HPT has been designed for a high hammering frequency f_{HP}, which shall correspond to a resonance frequency of the whole system (process, HPT and the actuator). The resonance frequency also depends on the workpiece properties. This implies a possible difference of resonance frequencies for different workpieces. For the purpose of adjustable resonance frequency, the stiffness of the HPT has to beadjustable as well. The variation of the stiffness is performed by using a ring spring, as shown in Figure 2. The ring spring is fixed to a gear wheel at two opposite positions. Furthermore, there are two moveable clamped joints whose position determines the stiffness of the tool. Ifthe clamped joints are arranged near to the ring spring fixation, a high stiffness value

is reached. In contrast to that, if the clamped joints are in the middle of the distance between the two fixations, the tool features the lowest stiffness value. The position of the clamped joints is changed by a step motor with a gear (see Figure 2). The piezoelectric actuator is placed coaxial with the axis of the HPT and it is connected to the base disc as well as to the plunger with the ball on its upper and lower part, respectively. In order to make the piezoelectric actuator free from radial forces, the movement is guided in upper and lower guidance in form of flexure hinges. The tool can be fixed in a machine tool or in a robot via the tool-interface.

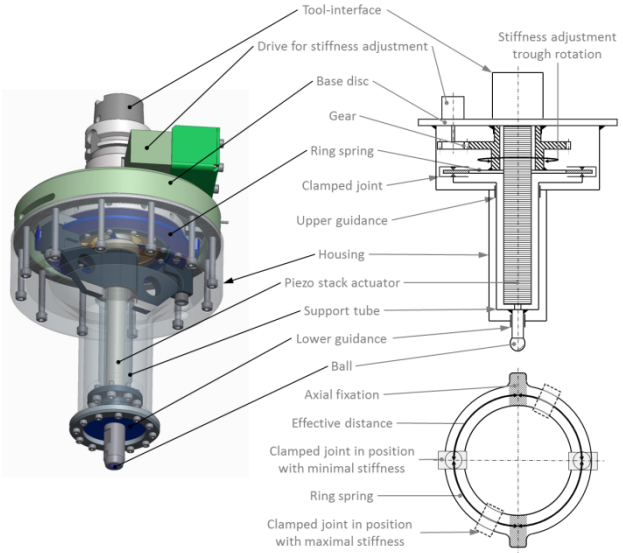

Figure 2. Scheme of piezo-actuated hammer peening tool with adjustable stiffness

The piezoelectric actuator is actually a piezo stack actuator consisting of many piezoelectric disks utilizing the longitudinal effectfor a relatively high stroke of 0.2 mm. The maximal blocking force of the actuator amounts to 4000 N. Since the actuator is preloaded, a pull loading with maximal value of 700 N is acceptable. The length and diameter are 185 mm and 18 mm, respectively. The first resonance frequency of the actuator approximately amounts to 3 kHz.

3 CROSS-DOMAIN MODEL

The development of the piezo-actuated HPT and of the hammer peening technology is connected to a relevant model of the whole system including thehammer peening process,the structural mechanics as well as the electric domain of the HPT. For this purpose, a cross-domain dynamic model has been developed.Moreover, such a model in combination with experimental results allows a further optimization of the piezo-actuated HPT regarding its productivity, lightweight design and reliability.

The modelling approach presented in this paper integrates the electric domain into a structural mechanic model using the analogy between mathematical formulation for an electric and mechanical oscillator, as expressed in eq. (2) for linear systems

$$\begin{aligned} \mathrm{m}\ddot{x}(t)+\mathrm{b}\dot{x}(t)+\mathrm{k}x(t)&=f(t) \\ \mathrm{L}\ddot{q}(t)+\mathrm{R}\dot{q}(t)+{}^{1}\!/_{\mathrm{C}}\,q(t)&=u(t) \end{aligned} \tag{2}$$

in which the constants m, b, k, L, R and C denotethe inertial mass, damping constant, static stiffness, electrical inductance, el. resistance and el. capacitance, respectively. Moreover,the variables:*x*, *f*, *q* and *u* represent displacement, force, el. charge and voltage, respectively. Eq. (2) yields the analogy between the two domains in the form of: $x \Leftrightarrow q$, m ⇔ L, b ⇔ R, k ⇔ 1/C, $f \Leftrightarrow u$. The electric domain contains the electric properties of the used piezoelectric actuators as well as its driver electronics. Assuming a very high impedance of the driver electronics, the electro-mechanics of the piezoelectric actuators can be modelled in accordance with [Schugt 2001], [Wittstock 2006], as depicted in Figure (3).

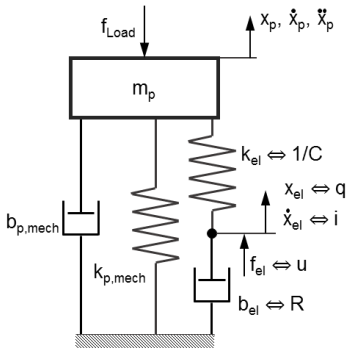

Figure 3. Linear rheologic model of a piezoelectric actuator

In this model, the parameter m_p represents the effective mass of the piezo stack actuator. It is actually a part of the mass of the piezo stack actuator being accelerated during vibration. Furthermore, the parameters $b_{p,mech}$ and $k_{p,mech}$ stand for the mechanical properties of the piezo stack actuator like damping constant and the static stiffness. The remaining parameters, i.e. b_{el} and k_{el}, include the electric properties of the piezo stack actuator and its driver electronics into the linear rheological model by using the electro-mechanical analogy.The model presented in Figure (3) has two degrees of freedom. The first one, depicted by x_p, is the displacement of the piezo stack actuator. The second one is an internal degree of freedom of the piezo stack actuator resulting from the electrical domain. As loading under tension of the piezo stack actuator has to be avoided, the resulting load f_{load} is depicted in Figure 3 as a compressive force. The active force inducing the displacement of the piezo stack actuator f_{el} results from the inverse piezoelectric effect. Assuming linear behaviour and the fact that the mechanical stress acts on the same area as the electrical field, the force f_{el} can be computed as follows

$$f_{el} = \alpha_{\mathrm{p}} u = \frac{\mathrm{d}_{33}\mathrm{C}_{\mathrm{p}}}{\mathrm{s}_{33}^{\mathrm{E}}\varepsilon_{33}} u \tag{3}$$

with C_p, d_{33}, s^E_{33} and ε_{33}being the el. capacitance of the piezo stack actuator,the piezo modulus, the Young's modulus and the permittivity of the piezo ceramic for the longitudinal piezo effect, respectively. These two parameters can be synthesized to one proportionality factor α_p.

The mechanical stiffness $k_{p,mech}$ of the piezo stack results from

$$\mathrm{k}_{\mathrm{p,mech}} = \frac{\mathrm{A}_{\mathrm{p}}}{\mathrm{s}_{33}^{\mathrm{E}}\mathrm{l}_{\mathrm{p}}} \tag{4}$$

where A_p and l_p are the cross-section area and the length of the piezo stack, respectively. The electrical stiffness k_{el} is computed as

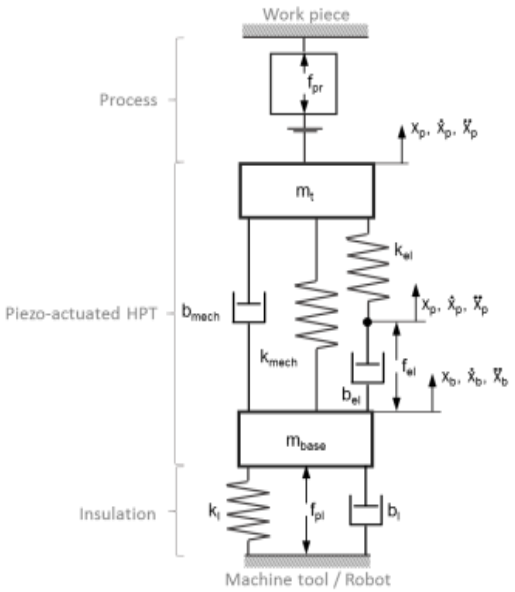

Figure 4. Dynamic cross-domain model for hammer peening with piezo-actuated HPT

$$k_{el} = \frac{A_p}{\left(\frac{s_{33}^E \varepsilon_{33}}{d_{33}^2} - 1\right) s_{33}^E l_p} \tag{5}$$

Furthermore, the el. damping corresponds to the inner el. resistance R_i of the piezo stack in accordance with the following equation

$$b_{el} = \alpha_p^2 R_i \tag{6}$$

This model can be further extended to the desired cross-domain model by adding the process, the insulation model and the mechanics of the HPT in accordance with Figure 4. In this model, the complete mechanical stiffness k_{mech} and damping constant b_{mech} of the HPT are integrated. They represent the sum of the mechanical stiffness or mechanical damping constant of the piezo stack actuator $k_{p,mech}$ or $b_{p,mech}$, of the support tube and the adjustable stiffness of the ring spring. Furthermore, the mass $m_t$is the massof the moving part of the HPT including the mass m_p. This point corresponds to the tool centre point (TCP). Assuming a very high stiffness between the piezo stack actuator and the ball, the movement of the ball (TCP) can be denoted as x_p.

The insulation model represents a part located between the HPT and the machine with a defined mechanical stiffness k_I,a damping constant b_I and an exerted static preload f_{pI}. These parameters are important for the effective operation of the HPT, as explained in sec. 5.

The purpose of the process model consists in reproducing the properties of the workpiece regarding its elasticity and plasticity. Furthermore, a contact between the ball and the workpiece, which changes its status between opened and closed during hammer peening, is also considered (in Figure 4 depicted by the two parallel horizontal lines). In order to model the plasticity and elasticity of the workpiece, the linear Kelvin-Voigt model is used here. The elasticity can be perceived as an energy accumulator and the plasticity as the work done for the remaining deformations. In this manner, the elasticity can be modelled by a spring and the plasticity by a damper. For the purpose of determining of these two parameters, finite element (FE) simulations have been performed, as shown in Figure 5.

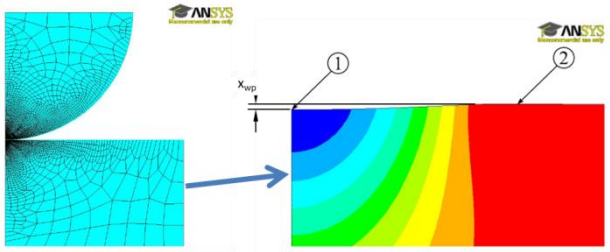

Figure 5. FE-model and post-processing of results

In these simulations, the process force f_{pr} and the corresponding deformation x_{wp} were evaluated for different materials (Aluminium-alloy, carbon steel, complex phase steel). The numbers 1 and 2 in Figure 5 depict the zone of the maximal deformation (the centre of the contact) and the area with material accumulation, respectively. The evaluated results are shown in Figure 6. In this figure, the process starts at the origin. Generally, the function $f_{pr} = f(x_{wp})$ is nonlinear and there is a significant hysteretic effect. These functions are nearly independent on the frequency in the range of interest (< 1 kHz). Therefore, linear Kelvin-Voigt model with structural damping is used for the simulation of the process. The constantparameters of the process model are identified by using these functions and an energetic approach. For this purpose, the accumulated energy corresponding to the remainingelastic energy W_e and the total energy for one hit of the hammer peening process W_t are computed as follows

$$W_e = \frac{f_{pr,\max}\left(x_{wp,\max} - x_{wp,res}\right)}{2}$$
$$W_t = \frac{f_{pr,\max} x_{wp,\max}}{2} \tag{7}$$

The difference of these two energy values yields the work done for the plastic deformation $W_p = W_t - W_e$. The parameter of the Kelvin-Voigt model determining the elasticity results from

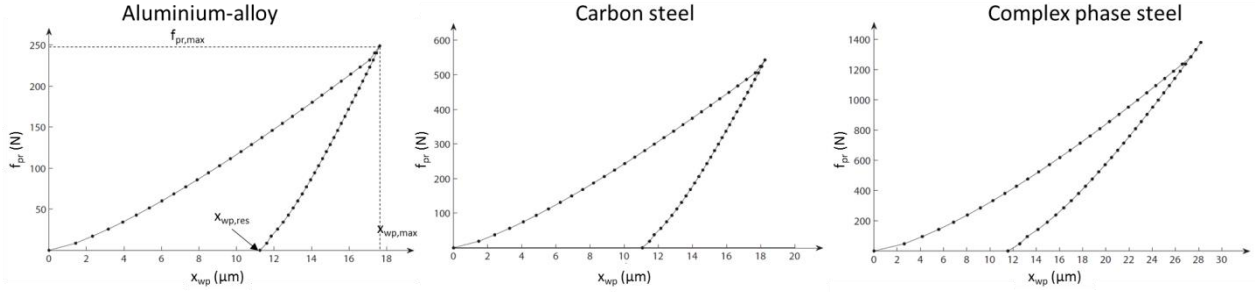

Figure 6. Process force f_{pr}as a function of the penetration x_p during contact resulting from FE analysis

$$k_{pr} = \frac{2W_t}{x_{wp,\max}^2} \tag{8}$$

The parameter of the linear Kelvin-Voigt modelbeing responsible for the plasticity is computed form the area of the hysteretic curve. This area corresponds to the plastic deformation. For this purpose, this area is assumed to have elliptic shape. The related damping parameter is computed in a closed-ended form as

$$b_{pr} = \frac{W_t - W_e}{\omega_{HP} x_{p,\max}^2 \left[t_{ret}/2 + \sin(2\omega_{HP} t_{ret})/4\omega_{HP} \right]} \tag{9}$$

In eq.(9), $\omega_{HP} = 2\pi f_{HP}$ and $t_{ret}$is the time, that the tool needs for leaving the workpiece.
The results are summarized in Table 1 for the three materials and frequency f_{HP} of 1 kHz.

	Aluminium-alloy	Carbon steel	Complex phase steel
k_{pr}	14045 N/mm	29121 N/mm	49110 N/mm
b_{pr}	6447 N/mm	12840 N/mm	14789 N/mm

Table 1. Identified parameters of the Kelvin-Voigt model, i.e. process model

4 IDENTIFICATION OF MODEL PARAMETERS FOR THE HAMMER PEENING TOOL

The parameters of the HPT like the mass m_t, the mechanical stiffness k_{mech}, the mechanical damping b_{mech}, the electrical stiffness k_{el} and the electrical damping b_{el} are crucial for the simulation results. Generally, the damping parameters are a prior unknown. Furthermore, the stiffness values are afflicted with uncertainties due to the contact problems as well as the variance of material characteristic values. Therefore, these parameters are estimated during an identification procedure. For this purpose, frequency response functions (FRF) are estimated from measured values. The first FRF (H_{xf}) describes the dependency of the displacement at TCP on the force acting on TCP, too. The second FRF (H_{xu}) is a function between the drive voltage of the piezo stack actuator as the input signal and the displacement at TCP as the output signal. Both FRFs are shown in Figure 7 at which H_{xu} is estimated for voltage amplitudes from 1.25 V to 30 V. In contrast to the first FRF, these results indicate a nonlinear behavior of the system. The nonlinearities can origin from the electromechanical behavior of the piezo stack actuator as well as from the clamped joints on the ring spring (see Figure 2). Unfortunately, it is not possible to distinguish between these two sources for nonlinearities with the used measurement set up. Therefore, the mechanical stiffness is assumed to be responsible for the nonlinearity and it will be modelled with a linear and nonlinear part as follows

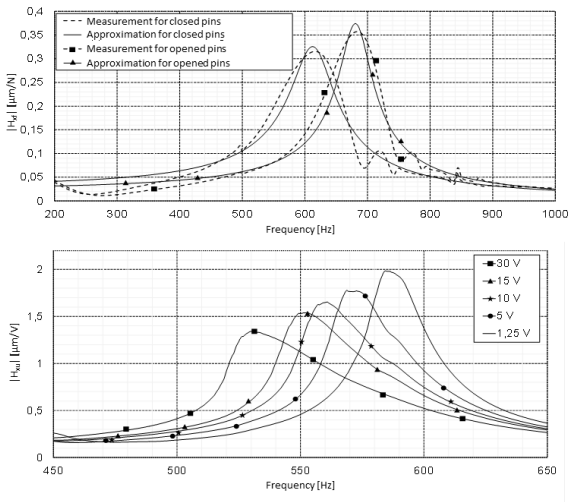

Figure 7. Experimental estimated FRFs for the piezo-actuated HPT

$$k_{mech} = k_{mech,nl} x_p^{\kappa} + k_{mech,l} \tag{10}$$

In order to model a correct damping ratio independently on the nonlinear elasticity, the damping constant must also be nonlinear.

$$b_{mech} = b_{mech,nl} x_p^{\chi} + b_{mech,l} \tag{11}$$

The first FRF, i.e. H_{xf}, is utilized for the first estimation of the start parameters in the identification. The measurement with closed pins of the piezo stack actuator enables the estimation of the mechanical values like $k_{mech,l}$ and $b_{mech,l}$. Assuming that the mass m_t is sufficiently known from the CAD model of the HPT, the mechanical stiffness $k_{mech,l}$can be computed from the resonance frequency. Afterwards, the damping constant $b_{mech,l}$is determined from the measured damping ratio θ.

$$b_{mech,l} = \theta 2\sqrt{k_{mech,l} m_t} \tag{12}$$

Furthermore, the electrical stiffness k_{el} can be computed from the difference of the resonance frequencies between measurements for closed and opened pins of the piezo stack actuator when the influence of the damping on the resonance frequency is neglected. The value for the electrical damping b_{el} was estimated from experience.
The second FRF H_{xu} is utilized for the reference in the identification procedure. The identification is based on the following optimization task

$$\min\left\{ J(\mathbf{p}) = \sum_{I} \left(H_{xu}^{M}(\omega_i, \mathbf{p}) - H_{xu}^{S}(\omega_i, \mathbf{p}) \right)^2 \right\} \tag{13}$$

in which the superscripts M and S denote the measured and simulated FRF, respectively. The optimization is performed over a frequency range I, i.e. from 450 Hz to 650 Hz. The parameter vector **p** contains the model parameters to be identified, i.e. $\mathbf{p} = \{m_t k_{mech,l} k_{mech,nl} b_{mech,l} b_{mech,l} k_{el} b_{el} \kappa \chi\}^T$. The procedure for the identification is schematically pictured in Figure 8.

Parameter	Start value	Lower limit	Upper limit	Optim. value
b_{el} (Ns/m)	30	25	40	**31**
k_{el} (N/µm)	7	6.6	7.2	**6.7**
$k_{mech,l}$ (N/µm)	24	22	27	**25.3**
$k_{mech,nl}$ (N/µm²)	-0,1	-2	0	**-0.6**
$b_{mech,l}$ (Ns/m$^{1+\kappa}$)	300	130	450	**210**
$b_{mech,nl}$(N/µm$^{1+\chi}$)	10	0	15	**7**
κ	1	0.2	2	**0.6**
χ	1	1	2	**1.35**

Table 2. Setting of the model parameters for the identification and the identified model parameters

The results of the identification are summarized in Table 2. This table contains the start values for the model parameters and the set upper and lower limits during the identification. In the last column, the optimized values of the model parameter are listed. It can be seen that the optimized values differ from the start values in a relatively low level. This implies that the relatively simple determination of the startvalues already yielded good estimation for the model parameters disregarding the nonlinearities. In order to proof the model accuracy including the nonlinearities, a comparison between measured and simulated H_{xu} for two voltage amplitudes, indeed 5 V and 30 V, is shown in Figure 9. It can be seen that a very good correlation between measured and simulated values exists.

Simulation run no.	Preload / gap	k_l
1	300 N	1 N/mm
2	300 N	10 N/µm
3	0 N / 0 µm	1 N/mm
4	0 N / 0 µm	10 N/µm
5	20 µm	1 N/mm
6	20 µm	10 N/µm

Table 3. Parameters of the insulation unit matched to simulation runs

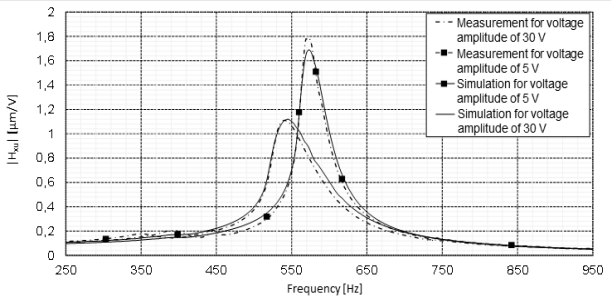

Figure 9. Comparison between measured and simulated results after the identification

5 SIMULATION OF THE HAMMER PEENING PROCES

After the process models as well as the model of thetool are ready for simulation, various simulation runs of hammer peening can be carried out in order to study the parameters of the insulation model. The damping properties of the insulation model are defined by the damping ratio $\vartheta$with assumed value of 5%. The simulations are performed for various configurations of parameters according to Table 3. The simulation results shall yield a basic overview of an appropriate parameter setting of the insulation unit (model). For this purpose, two values for the stiffness k_l are chosen. The high value of 10 N/µm approximately corresponds to a stiffness value of a machine tool. This value implies that an insulation unit is not necessary for the hammer peening with a piezo actuated tool. In contrast to this, the low stiffness valuenearly equates to a mechanical decoupling between the HPT and the machine/robot. This would lead to hammer peening process with a piezo actuated tool regardless of the used machine.

Beside the stiffness, the static preload is also considered in the study. For this purpose, three states are defined here. The first one represents hammer peening with a piezo actuated tool under static preload. The value of the static preload amounts to 300 N. The second state represents a closed contact between the HPT and the workpiece without any static preload. This state is purely theoretic since deviations from the ideal workpiece dimensions or shapes as well as from thetool path due to the machine inaccuracy leads either to a gap or to a static preload depending on the stiffness k_l. The last state assumes an initial gap of 20 µm between the HPT and the workpiece. This state has a low relevance for the praxisdue to the same reasons as in case of the second state.

The simulation runs were performed with a chirp signal changing its frequency linearly from 0 Hz to 1500 Hz during 15 s. Therefore, a rough correlation between the time domain and the frequency domainis possible, i.e. 1 s on the time axis corresponds to 100 Hz on the frequency axis. Thus, the investigation in frequency domain can be performed despite the nonlinearityin the process model.

The simulation results are summarized in Figure 10 for all three materials(Aluminium-alloy, carbon steel, complex phase steel). In this figure the displacement of TCP x_p is evaluated. Generally, the positive valuesof $x_p$or values greater than the gap represent the penetration of the HPT into the workpiece, in Figure 10 depicted as x_{pen}. In case of the simulation run no. 5 and 6, the penetration starts at x_p = 20 µm due to the gap. For a smoothing effect, a large value of penetration is desired. Furthermore, the negative range of $x_p$means that the contact between HPT and the workpiece is opened, i.e. the HPT takes off from the workpiece. This value is denoted as x_{toff}. The value has to be negative or lower than the gap. In other case, the ball

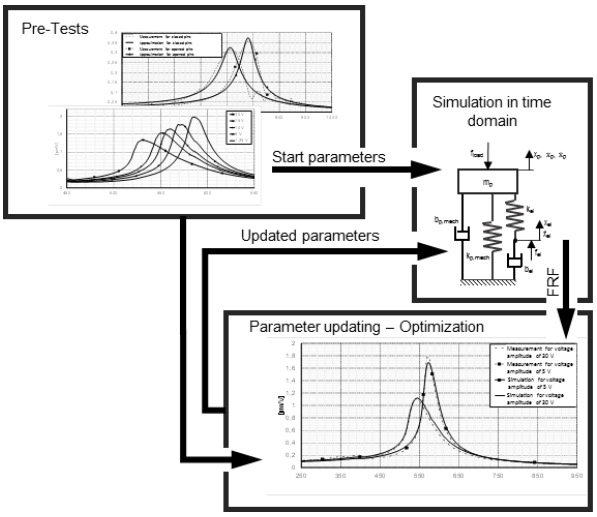

Figure 8. Procedure for the identification of the model parameters of the piezo-actuated HPT

of the HPT remains inside of the workpiece and the ball pressed a groove on the surface instead performing hits. Therefore, the condition for $x_{toff}$is crucial for the hammer peening process. Moreover, the hits on the surface have to be performed with the frequency of the drive voltagef_{dv} in order to reach a high productivity. As one can see in Figure 10 at the simulation run no. 3 and 5, there is a difference between the frequency of the drive voltage and the hammer peening frequency f_{HP} in wide frequency ranges. Exemplary for simulation run no. 3, the condition of $f_{dv} = f_{HP}$ is only satisfied in a narrow frequency range approximately between 550 Hz and 600 Hz. In this frequency range, the resonance frequency is located. Outside of this frequency range, the HPT jumps on the surface like a ball with significantly lower frequency f_{HP}. For the sake of completeness, the condition for the f_{HP} is not fulfilled over the whole frequency range in case of the simulation run no. 5. In face to the two conditions, i.e. $x_{toff}< 0$ or $x_{toff}<$ gap and $f_{HP} = f_{dv}$, the evaluation of the results can be carried out. The simulation run no. 5 can be excluded from the evaluation due to the violating the frequency condition. Furthermore, the simulation run no. 1 fulfils the condition regarding the x_{toff}only for the complex phase steel or in two very narrow frequency ranges in case of the carbon steel. Generally, the hammer peening frequency f_{HP} in simulation run no. 1 for all materials corresponding to maximal penetration is located significantly under the resonance frequency.Considering the frequency of a pneumatic HPT, there would not bea benefit of the piezo-actuated HPT for the productivity in this case. Therefore, the parameter setting for the simulation run no. 1 is not appropriate for the piezo-actuated HPT. The simulation run no. 3 features a narrow frequency range around the resonance frequency with the fulfilled frequency condition. However, the valuex$_{toff}$ is very large in this frequency range whichexceeds the movement range of the piezo stack actuator of 0.2 mm (see sec. 2). Therefore, this setting is also not appropriate for the piezo-actuated HPT. The last three simulation runs (no. 2, 4 and 6) yield good results, for which therealisation of the hammer peening process with the piezo-actuated HPT seems to be possible regardless the workpiece material. From the practical point of view, the simulation run no. 1 owns the highest relevance. In this case, the influence of deviations from the ideal tool path and the ideal workpiece on the preloading and thus on the process should be considered. The big differences between results of simulation run no. 1,2 and 3 indicate the large influence of the static preload and the static stiffness $k_I$on the hammer peening process. Therefore, the further investigation should focus on this issue.

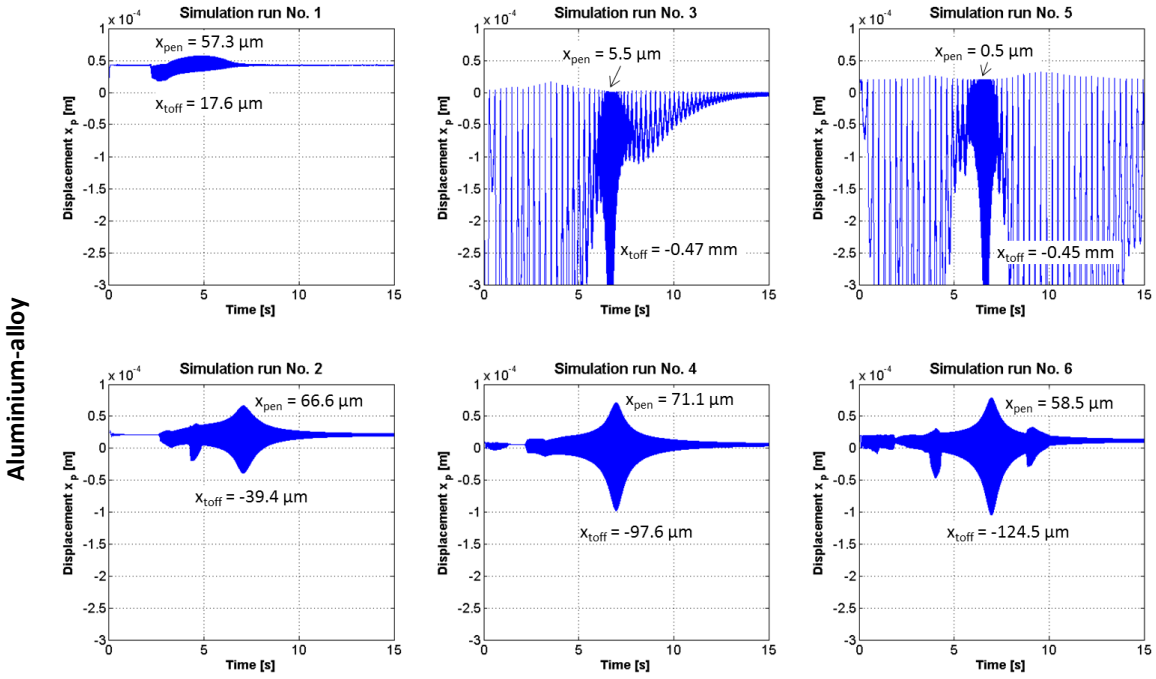

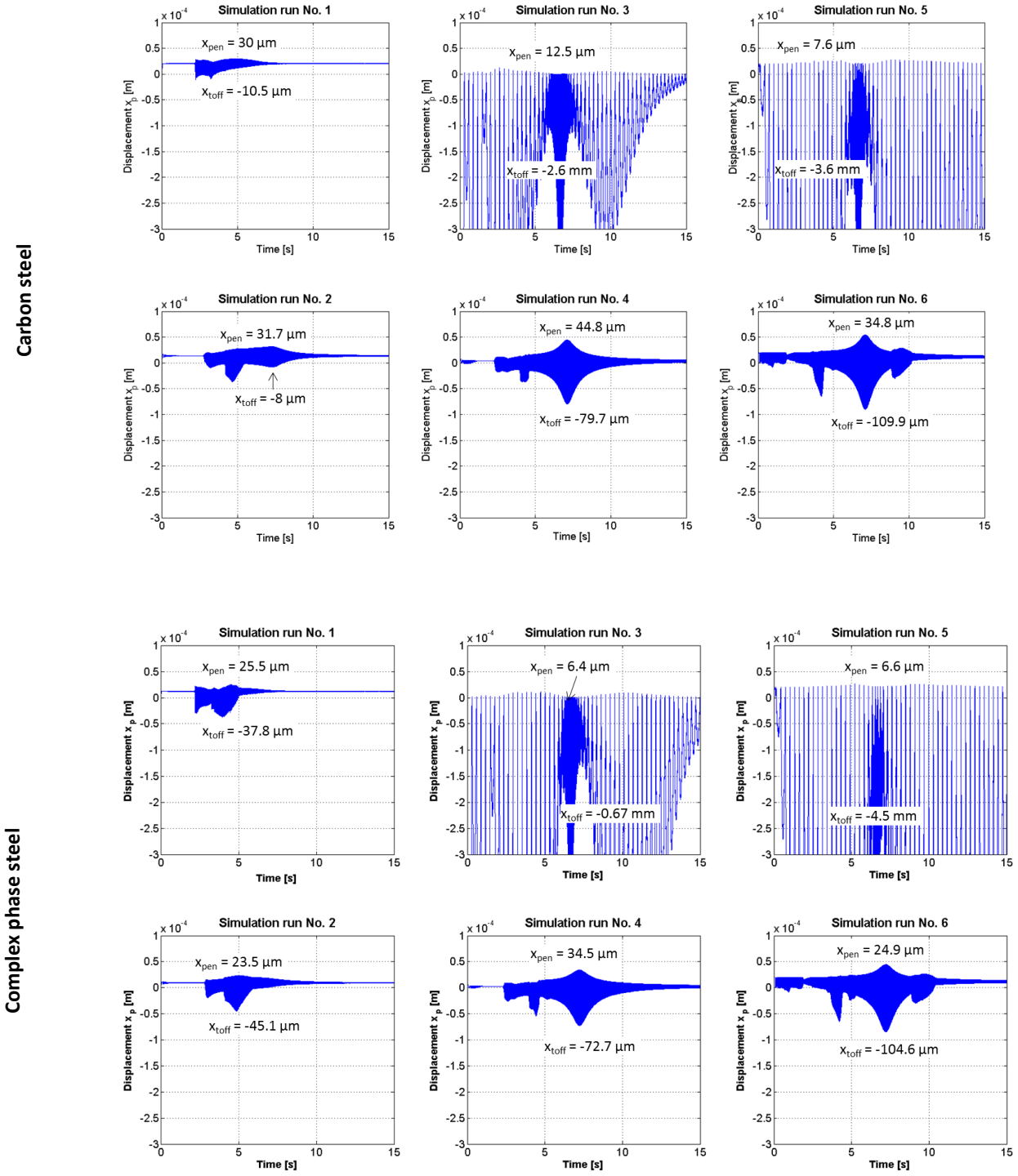

Figure 10. Simulation results for the displacement of TCP

6 MACHINING TEST WITH PIEZO-ACTUATED HAMMER PEENING TOOL

In order to demonstrate the capability of the piezo-actuated HPT for smoothing roughness of surfaces, a hammer peening process with the piezo-actuated HPT is carried out in this section. For this purpose, a plane surface is machined. The surface was milled and the initial roughness of this surface amounts to Rz 10 µm. The HPT is clamped in the spindle of a milling machine, as shown in Figure 11.

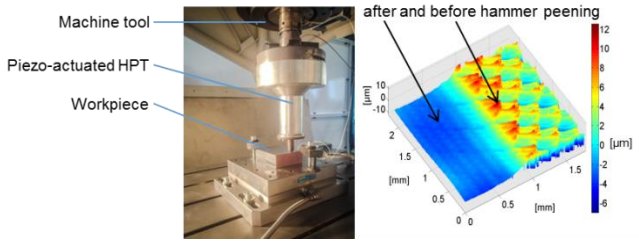

Figure 11. Machining test of the HPT and the roughness of the machined surface

In this machining test, a gap between the workpiece and the HPT is set to 35 µm with a very high effort.The piezo stack actuator is driven by the voltage amplitude of 130 V at the resonance frequency of the HPT, i.e. f_{dv} = 565 Hz. For these parameters, the plane surface after the hammer peening process featuresa roughness of Rz 1 µm. This value corresponds to roughness machinedby grinding or polishing. Thus, the hammer peening with the piezo-actuated HPT is able to be used for finishing of milled surfaces.

7 CONCLUSION AND OUTLOOK

In this paper, a novel piezo-actuated hammer peening tool is presented. The resonance frequency of this tool can be adjusted depending on the properties of machined workpiece. The operation of the tool at the resonance frequency increases the productivity and reduces the energy demand. Furthermore, a cross-domain model including the process, electro-mechanical properties of the tool and the coupling the tool to a machine by using an insulation unit is also presented. The a priori unknown model parameters or model parameters with high uncertainties are identified by using experimental results. Beside this, the process parameters are adopted from FE simulations. In this way, a very good correlation of the model and the experimental results is reached. Simulation results for different process settings are presented here. It is shown that the piezo-actuated hammer peening tool is able to work under a static preload in order to avoid the influence of inaccuracies of machine and workpiece.

The further works focus on optimization of the tool for reducing its dimensions and weight. Furthermore, new approaches are developed with that process parameters with high productivity and process stability can be quickly determined. Moreover, the parameters of the insulation unit are also investigated in order to utilize the piezo-actuated hammer peening tool for machining with robots. Last but not least, strategies for generation of the tool path are developed too.

REFERENCES

[Adjassoho 2012] Adjassoho, B. et al. Induction of residual stress and increase of surface hardness by machine hammerpeeningtechnology, Proceedings of the 23rd International DAAAM Symposium, 2012, Vol. 28, pp 697-702.

[Berglund 2011] Berglund, J., Liljengren, M., Rosen, B.-G. On finishing of pressing die surfaces using machine hammerpeening, The International Journal of Advanced Manufacturing Technology, 2011, Vol. 52, pp 115-121.

[Bleicher 2012] Bleicher, F. et al. Mechanism of surface modification using machine hammer peening technology, CIRP Annals - ManufacturingTechnology, 2012, Vol. 61, pp 375-378.

[Groche 2012] Groche, P. Potential of mechanical surface treatment for mould and die production, International Journal of MaterialsResearch, 2012, Vol. 102, pp 783-789.

[Groche 2011] P. Groche,P. Steitz, M. Prozess kettenverkürzungim Werkzeugbau, Werkstattstechnik online, 2011, Vol. 101, pp 655-659.

[Groche 2009] Groche, P. et al. Optimierung des Abrieb- und Verschleißverhaltens von Werkzeugoberflächen durch Randschichtverfestigung, EFB-Forschungsbericht Nr.296, 2009.

[Schugt 2001] Schugt, M. Aktor-Sensor verhalten von Piezoelementen in Kfz-Diesel-Einspritzsystemen. Ph.D.-Thesis, Bochum University, Department for electrical and information engineering, 2001.

[Wied 2011] Wied, J. Oberflächen behandlung von Umformwerkzeugen durch Festklopfen, Ph.D.-Thesis, Darmstadt University of Technology, 2011.

[Wittstock 2006] Wittstock, V. Piezobasierte Aktor-Sensor-Einheiten zur uniaxialen Schwingungskompensation in Antriebs strängenvon Werkzeugmaschinen. Ph.D.-Thesis, Chemnitz University of Technology, Department for mechanical engineering, 2006.

CONTACTS:

Dr.-Ing. Martin Kolouch, Ph.D.
Dipl.-Ing. Markus Wabner
Robin Kurth, M. Sc.
Fraunhofer Institute for Machine Tools and Forming Technology IWU,
Reichenhainer Strasse 88, 09126 Chemnitz, Germany
+49-371-5397-1362, Martin.Kolouch@iwu.fraunhofer.de
+49-371-5397-1458, Markus.Wabner@iwu.fraunhofer.de
+49-371-5397-1490, Robin.Kurth@iwu.fraunhofer.de
http://www.iwu.fraunhofer.de/